

Nonlinear Analysis of a Reactor Building for Airplane Impact Loadings

Th. Zimmermann, C. Rodriguez

*Motor-Columbus Consulting Engineers, Inc.,
Parkstr. 27, CH-5401 Baden, Switzerland*

B. Rebora

*IENER, Institut d'Economie et d'Aménagements Energétiques,
Swiss Federal Institute of Technology,
CH-1015 Lausanne, Switzerland*

SUMMARY

The purpose of this article is to analyze the influence of material nonlinear behavior on the response of a reinforced concrete reactor building and on equipment response for airplane impact loadings. Two analyses are performed: first, the impact of a slow-flying commercial airplane (Boeing 707), then the impact of a fast flying military airplane (Phantom).

Loads are simulated using prescribed load-time-histories. Nonlinear material behavior is restricted to the reactor building.

The material model accounts for a nonlinear stress-strain equation including isotropic hardening, multiaxial cracking and crushing in concrete. An elastic-plastic stress-strain relationship coupled with kinematic hardening is used for reinforcement steel.

The mathematical model is briefly described first. It consists of a finite element model. Space discretization is done using three-dimensional higher order isoparametric elements for concrete, membrane and truss elements for steel. Time discretization uses an implicit Newmark algorithm. The solution of the nonlinear equation of motion is obtained iteratively using the "initial stress" technique.

Second, the analysis of the impact of a Boeing 707 is performed and response spectra are established. This type of impact induces only moderate nonlinearities. Response spectra resulting from the nonlinear analysis show an increase in amplitude close to the impact location which vanishes away from the impact zone.

Third, the analysis of the impact of a Phantom is performed. This impact load induces a punching shear failure. The thrust transmitted to the undisturbed part of the structure shows a reduction due to material nonlinearity which is, however, associated with severe local damages.

Last, conclusions are drawn and the main hypotheses are discussed.

1. INTRODUCTION

Much work has been devoted during recent years to the analysis of response of safety-relevant structures to airplane impacts /1 - 10/. In some European countries, this type of loading has even become the most critical for design of reactor buildings.

For convenience, a distinction is usually made between the actual structural response, analyzed by finite element techniques, and equipment response, approached via floor response spectra analysis. Both aspects are analyzed in this article with special emphasis placed on the influence of taking into account material nonlinearity (concrete crushing and cracking, steel yielding) on structural response and on induced vibrations.

Interest in induced vibrations for airplane impacts started with articles of Sharpe & al. /1/ and Schaik & Wölfel /2/, which showed higher response spectra values than for SSE. This motivated research work which was intended to prove that taking material nonlinear behavior (in the impact zone) into account should reduce response spectra. Arguments along these lines have been presented by Kaiser & al. /3/, Krutzik /4/, Kamil & al. /5/, Schnellenbach & Stangenberg /6/. On the other hand, Wolf & al. /7/ established that for a high resistance ratio (yielding moment/maximum elastic moment), an amplification of response spectra should be expected, if a failure mechanism takes place. This conclusion was based on calculations using beam models.

Herein, three-dimensional nonlinear finite element analysis results are presented, for both the impact of a Boeing 707 and a Phantom on a reactor building initially designed for a Boeing impact. In a first step, the structural response is analyzed and the type of failure, if any, is identified. In this part, the approach proposed in an earlier article (Rebora & al. /8/) is followed. In a second step, induced vibrations are studied, via response spectra for the Boeing impact and via transmitted thrust for the Phantom analysis.

The impacting airplane is simulated by a load-time-history established following Riera /9/ for the Boeing impact and Drittler & Gruner /10/ for the Phantom. The target is assumed rigid. Discussion of hypotheses in relation with the load-time-history is beyond the scope of this article and can be found in References /7, 9, 10/. Since regulatory guidelines prescribe the load-time-history, the only aspect which deserves further attention is the influence of nonlinearity. This is discussed at some length in the sequel.

First a short description of the finite element model is given. Then, the vertical impact of a Boeing 707 on the top of the dome of the reactor building is analyzed. The same impact configuration is used, later on, for the Phantom analysis. Finally, conclusions are drawn which stress differences in nonlinear structural response for different impacting airplanes and the influence of material nonlinearity on induced vibrations.

2. FINITE ELEMENT MODEL FOR REINFORCED CONCRETE

A detailed description of the finite element model "TRIDI" is given in Zimmermann & Rebora /11/ and a summary is given in References /8, 12/. The code consists of a development with extension to dynamics of the model pioneered by Saugy /13/.

Particular features of the modelization are:

- Distinct simulation of concrete (discretized with 60-DOF isoparametric elements)

and steel (using 24-DOF degenerated membrane and 9-DOF truss elements). No bond slip effect is accounted for.

- The material model for concrete is based on nonlinear small strain elasticity. Isotropic hardening is included. Failure (both compressive and tensile) is characterized by a failure surface in stress-space.
- The material model for steel combines a bilinear stress-strain law with a Von Mises yield criterion and kinematic hardening.
- The nonlinear equation of motion is solved using Newmark's algorithm for time discretization and the initial stress technique for the iterative procedure.

3. AIRPLANE IMPACTS ANALYSES

Vertical impacts onto the top of the reactor dome are analyzed for both a Boeing 707-320 flying at 103 m/s and a Phantom RF-4E flying at 215 m/s (Fig. 1).

3.1 Boeing Impact

The main emphasis is placed on the influence of material nonlinearity in the impact zone on response spectra. This conditions the time step, chosen equal to 2 ms for an adequate mode representation up to 80 Hz. Also, since mainly qualitative results are wanted, the modeling is limited to a shell sector with radiating boundary conditions.

The load is defined by a prescribed load-time-history (Fig. 2a). The total duration of analysis is 400 ms. The geometry is given on figure 2b. It consists of a shell sector of radius 22 m (+ a boundary element) and of thickness 1.2 m. The finite element mesh is shown on figure 2c. It comprises 30 brick elements (concrete), 99 membrane elements (reinforcement steel). Material data are summarized in Table I.

Typical results are shown on figure 3. Principal stresses (defined at integration points by the intersection of the stress-ellipsoid with the plane of the figure) are plotted for two different times. At the maximum of the load (time t_a) cracking (shaded zones with lines parallel to crack traces) is essentially located at the intrados. After unloading (time t_b) cracking appears also at the extrados and within the shell. This cracking can be associated with the hysteresis phenomenon. No crushing (compressive failure), nor steel yielding is observed.

Figure 4 shows vertical acceleration-time-histories at locations A and B resulting from both linear and nonlinear analysis. It is observed that material nonlinearity increases acceleration amplitudes close to impact zone (Point A) but has little influence away from it (Point B). The high frequency vibration which appears (Point A) is due to an interference of the nonlinear iteration technique associated with cracking, and the time-stepping algorithm. It has no direct relation with a physical phenomenon. This point is subject to further discussion in articles by Zimmermann & al. /12, 14/, where it is stated that this noise has little influence on the response spectra in the frequency range of interest (below 80 Hz).

Figure 5 shows response spectra at locations A and B. It is observed that material nonlinear behavior induces a strong increase in response spectra close to the impact area, influence which disappears when moving away. As a consequence, the vertical shear force $F_v(t)$ transmitted to the undisturbed part of the structure (Fig. 6a) shows almost

no influence of material nonlinearity (Fig. 6b).

3.2 Phantom Impact

Our main goal here, is to determine whether or not this type of impact leads to a local failure. The time step (2.5 ms) is constrained by the condition that load increments should be small enough to allow a correct simulation of the nonlinear behavior.

The load-time-history is defined on figure 7a. The total duration of analysis is 70 ms. The geometry is shown on figure 7b. A sector of the complete shell is modeled. A special boundary element is introduced to account for the foundation. The mesh comprises 55 brick elements (some with reduced number of DOF), 48 membrane elements (mainly bending reinforcement), 76 truss elements (shear reinforcement bars). Material data are the same as for the first analysis except for : $\beta'_{pd} = -367.$, $\beta_t = 30.$, $\nu = 0.18$. These values were felt to be more realistic for the purpose of an ultimate load analysis. Data are summarized in Table II.

Figure 8a shows the concrete stresses, cracking and crushing patterns, and steel yielding. Again, cracks are represented by shaded spots. The shading lines density is proportional to crack opening, so that dark shading characterizes open cracks. It is observed that significant two-directional cracking occurs first at the intrados in the center and spreads out radially. Steel yielding appears first in shear reinforcement at $P = 0.75 P_{max}$. It propagates when $P = 0.875 P_{max}$. Also, crushing appears along the load edge. During the failure mechanism ($P > 0.875 P_{max}$) crack opening localizes along shear reinforcement bars, while cracks which do not participate in the mechanism tend to close. The strain in shear reinforcement reaches $\sim 1\%$ at this time step. Bending reinforcement yielding appears ultimately, both in radial and tangential directions. Some crushing also appears at the intrados. The observed mechanism corresponds to a punching shear failure, which is best observed on the velocity field of figure 8b. The mechanism corresponds to an expulsion of the central part of the shell, underlying the impact surface.

The vertical shear force transmitted to the undisturbed part of the structure is shown on figure 9. It is observed that the nonlinear analysis may lead to a reduction of the maximum shear force. This could result in lower maximum acceleration for response spectra. It should, however, be remembered that this reduction is associated with a failure mechanism. If such severe damages are not tolerable, the shell thickness should be increased. As a consequence, the favorable effect of material nonlinear behavior would disappear.

4. CONCLUSIONS

4.1 Boeing Impact Analysis

This load is characterized by a large ratio $d/h = 4.7$ (load diameter/shell thickness). For the specific structure (shell thickness 1.2 m) and data considered in this analysis, the impact of a Boeing 707 at 103 m/s induces only moderate damages: some concrete cracking, no crushing, no steel yielding. Failure initiation is of bending type. Material nonlinearity leads to an increase in the amplitude of response spectra in the immediate vicinity of the impact location. Away from the impact zone (~ 3 times the load diameter) effects of nonlinearity vanish. Since the structure is designed to withstand this

type of impact, significant material nonlinearity appears only close to the maximum load ($t = 0.214$ s). Therefore, only moderate local energy dissipation takes place.

4.2 Phantom Impact Analysis

This load is characterized by a smaller ratio d/h , equal to 2.5, and a higher maximum load. For the specific structure considered in this analysis, the same as for the preceding one, the impact of a Phantom induces punching shear failure at $P > 0.875 P_{max}$. If such severe local damages are allowed for, a possible reduction of the induced vibrations, due to material nonlinearity, could occur. The amplitude of such a reduction could not be established in the present analysis.

4.3 Discussion of Hypotheses

Load - The airplane impact loads are simulated by a prescribed time-history applied on a constant area. The target is assumed to be rigid and a simple deformation model /9/ is considered for the airplane. A posteriori, these assumptions appear admissible for the Boeing impact. For the Phantom impact, failure induces larger displacements so that the assumption of a rigid target is invalidated. The hypothesis of a constant impact area is conservative, if an average value is chosen.

Mathematical Model - The finite element model appears adequate. Difficulties arise in the high frequency range due to interaction of the time stepping algorithm with the modeling of cracks. This, however, has little influence in the frequency range of interest. Also, when failure occurs, convergence of the constant stiffness algorithm is much too slow, it should be replaced by an adequate variable stiffness algorithm.

Within the range of linear material behavior, the accuracy of the chosen Newmark scheme is established: no amplitude decay, moderate period elongation (~7 % at 50 Hz). This result can be extended to the range of moderately nonlinear behavior. The quality of the observed accelerations remains, at this point, an open question.

The Phantom impact analysis fails to converge for $P > 87,5 \% P_{max}$. Experience shows that divergence of the program "TRIDI" occurs above 80 % of the actual failure load, which sometimes overshoots the rigid-plastic theoretical solution. It is reasonable to consider the obtained ultimate load as a lower bound to the actual failure.

Boundary Conditions - The Boeing impact is analyzed on a local mesh. To be rigorous, interpretation of results should therefore be limited to relative values (linear vs. nonlinear). The Phantom impact is analyzed on a global model including foundation elements.

Material Data - Material data include stress-strain law and failure surface for concrete and yield criterion for reinforcement steel. Steel data are usually precisely known. Assuming the compression strength of concrete to be well defined, elastic moduli and tensile strength remain to be extrapolated. The moduli adopted in both analysis correspond to average values. Since the influence of nonlinearity of the stress-strain relation is small in both analysis, tensile strength is the only material characteristic which would require a sensitivity study.

Tensile strength influences crack initiation and, therefore, crack induced high-frequency vibrations. It has no significant influence in the frequency range of interest.

For bending type failure, in adequately reinforced members, tensile strength is unimportant. For punching shear failure, compression strength is dominant /15/.

4.4 Closure

From a detailed analysis of results obtained by the two studies reported herein, as well as earlier computations /8, 16/, it appears that the impact on this reactor building of a Boeing 707 (slow-flying, large impact surface) initiates a bending type failure. For a military airplane (fast-flying, small impact surface), a punching shear failure type tends to appear first, preceding (probably shortly) a bending failure. For a high resistance ratio (yielding/maximum elastic stress resultant), material nonlinearities will increase the amplitude of induced vibrations (and response spectra) close to the impact zone. At some distance, this effect will vanish; a reduction of amplitude of induced vibrations can only appear in conjunction with severe damages in the impact zone.

REFERENCES

- /1/ R. Sharpe, H. Kamil, R. Scanlan. Trans. 3rd Int. Conf. on Struct. Mech. in React. Technol., London, 1975, Paper J5/4
- /2/ M. Schalk & H. Wölfel. Nucl. Eng. Des. 38 (1976) 567
- /3/ A. Kaiser, N. Krutzik, K.-H. Schrader, G. Winkel. Trans. 4th Int. Conf. on Struct. Mech. in React. Technol., San Francisco, 1977, Paper J8/3
- /4/ N.J. Krutzik: Analysis of Aircraft Impact Problems. In "Advanced Dynamics", Ed. J. Donña, 1979
- /5/ H. Kamil, G. Kost, R. Sharpe. Preprint of ASCE Nat. Conv., Civil Eng. & Nucl. Power, Vol. III, 1979
- /6/ G. Schnellenbach, F. Stangenberg: Neue Entwicklungen bei der Auslegung von Kernkraftwerken gegen Flugzeugabsturz. VGB Kraftwerktechnik 59, Heft 1, 1979
- /7/ J.P. Wolf, K.M. Bucher, P.E. Skrikerud. Nucl. Eng. Des. 47 (1978) 169
- /8/ B. Rebora, Th. Zimmermann, J.P. Wolf. Nucl. Eng. Des. 37 (1976) 269
- /9/ J.D. Riera. Nucl. Eng. Des. 8 (1968) 415
- /10/ K. Drittler, P. Gruner. Nucl. Eng. Des. 37 (1976) 245
- /11/ Th. Zimmermann, B. Rebora: Three-Dimensional Nonlinear Dynamic Analysis with the Program "TRIDI". IENER Report 79.1
- /12/ Th. Zimmermann, B. Rebora, C. Rodriguez: Aircraft Impact on Reinforced Concrete Shells. Comp. & Struct., Vol. 13 (1981) 263
- /13/ B. Saugy: Contribution a l'étude théorique du comportement non-linéaire des structures massives en béton sous charges rapides. Bull. Tech. de la Suisse Romande No 22, 1969
- /14/ Th. Zimmermann, C. Rodriguez, B. Rebora: Nonlinear Analysis of a Reactor Building for Airplane Impact Loadings. Extended version of present paper, to be published
- /15/ M.W. Braestrup: Punching Shear in Concrete Slabs. Introductory report of the IABSE Colloquium - Plasticity in reinforced concrete, Copenhagen 1979.
- /16/ P. Degen, H. Furrer, J. Jemielewski. Nucl. Eng. Des. 37 (1976) 249

TABLE I : MATERIAL DATA (BOEING IMPACT)

Concrete	
$\beta_p = -240$ (β_p/cm^2) ($= 0.8 \beta_w = 0.8(-300)$) *	} strengths
$\beta_{pd} = 1.2 \cdot \beta_p = -288$ (kp/cm^2)	
$\beta_b = 1.2 \beta_p = -288$ -"	
$\beta_{bd} = 1.2 \beta_{pd} = -345.6$ -"	
$\beta_t = 2.5 \sqrt{ \beta_w } = 43.3$ -"	
$\beta_{td} = 1.2 \beta_t = 52$ -"	
$E_o = 19,000 \sqrt{1.2 \beta_w } = 3.6 \cdot 10^5$	} elastic moduli
$E_{od} = 1.1 E_o = 3.96 \cdot 10^5$	
$\nu_d = 0.2$	Poisson's coefficient
$\gamma_c = 2.5 (10^3 \text{kp}/\text{m}^3)$	specific mass
$\epsilon_r = 0.003$ uniaxial failure strain	
Bulk modulus $K = \frac{E_d}{3(1-2\nu_d)} = 2.2 \cdot 10^5$ (kp/cm^2)	
Initial shear modulus $\nu_o = \frac{E_d}{2(1+\nu_d)} = 1.65 \cdot 10^5$ (kp/cm^2)	
Shear modulus $\mu = \nu_o - \alpha \ln \frac{12}{12e}$, $\alpha = 0.596 \cdot 10^4$ (kp/cm^2)	
Steel	
$E_s = 2.1 \cdot 10^6$ (kp/cm^2)	Reinforcement
$E_s' = 2 \cdot 10^4$ (kp/cm^2)	
$\sigma_y = 4,600$ (kp/cm^2)	Bending**: 50,26 cm^2/m (radius = 0 to 78,54 cm^2/m (radius = 22 m)
$\beta_s = 5,600$ (kp/cm^2)	Shear: 16 $\#$ 18/m ² (40,8 cm^2)
$\gamma_s = 7.85$ (t/m^3) (set to $\gamma_s = 0$)	
Subscripts:	
* p = prism, d = dynamic, w = cube, b = biaxial, o = initial, t = traction,	
r = rupture, c = concrete, e = limit of linearity, s = steel	
** upper, lower, radial and tangential (equal for simplicity)	

TABLE II : MATERIAL DATA (PHANTOM IMPACT)

Concrete	
Values at 28 days	
$\beta_p = 0.85 \beta_w = 0.85 (-300) = -255$ (kp/cm^2) *	} strengths
$\beta_{pd} = 1.2 \cdot \beta_p = -306$ "	
$\beta_{bd} = 1.2 \cdot \beta_{pd} = -367$ "	
$\beta_t = (2.5 + 3.0) \sqrt{ \beta_w } = 43.3 + 52.0$ "	
$\beta_{td} = 1.2 \cdot \beta_t = -440$ "	
$E_o = 19,000 \sqrt{ \beta_w } = 3.29 \cdot 10^5$ "	} elastic moduli
$E_{od} = 1.1 \cdot E_o = 3.62 \cdot 10^5$ "	
$\nu = 0.18$	Poisson's coefficient
$\gamma_c = 2.5 \cdot 10^3$ (kg/m^3)	specific mass
$\epsilon_r = 0.003$	uniaxial failure strain
$\epsilon_{rd} = \epsilon_r$	
Values at two years	
$\beta_p' = 1.2 \cdot \beta_p = -306$ (kp/cm^2)	
$\beta_{pd}' = 1.2 \cdot \beta_{pd} = -367$ "	
$\beta_{bd}' = 1.2 \cdot \beta_{bd} = -440$ "	
$E_o' = 19,000 \cdot \sqrt{1.2/ \beta_w } = 3.6 \cdot 10^5$ "	
$E_{od}' = 1.1 \cdot E_o' = 3.96 \cdot 10^5$ "	
we adopt $\beta_t = 30$ kp/cm^2 , which corresponds to 0.1 β_p'	
Bulk modulus $K = \frac{E_{od}'}{3(1-2\nu)} = 2.06 \cdot 10^5$ (kp/cm^2)	
Initial shear modulus $\nu_o = \frac{E_{od}'}{2(1+\nu)} = 1.60 \cdot 10^5$ "	
Shear modulus $\mu = \nu_o - \alpha \ln \left(\frac{12}{12e} \right)$, $\alpha = 5.65 \cdot 10^4$ (kp/cm^2)	
"Boundary" element	
elasticity modulus = $E_o' d / 4.1 = 0.966 \cdot 10^5$ (kp/cm^2)	
specific mass = $\gamma_c \cdot 3.5 = 8.75 \cdot 10^3$ (kg/m^3)	
Steel	
$E_s = 2.1 \cdot 10^6$ (kp/cm^2)	
$E_{s2} = 2.0 \cdot 10^4$ "	(for $\sigma_s > \sigma_{sy}$)
$\sigma_y = 4,600$ "	
$\beta_{sr} = 5,600$ "	
$\gamma_s = 7.85 \cdot 10^3$ (kg/m^3) (set to $\gamma_s = 0$)	
* Subscripts: p = prism, w = cube, d = dynamic,	
b = biaxial, o = initial, t = traction, r = rupture, c = concrete,	
e = limit of linearity, ' = values at two years, s = steel, y = yield limit	

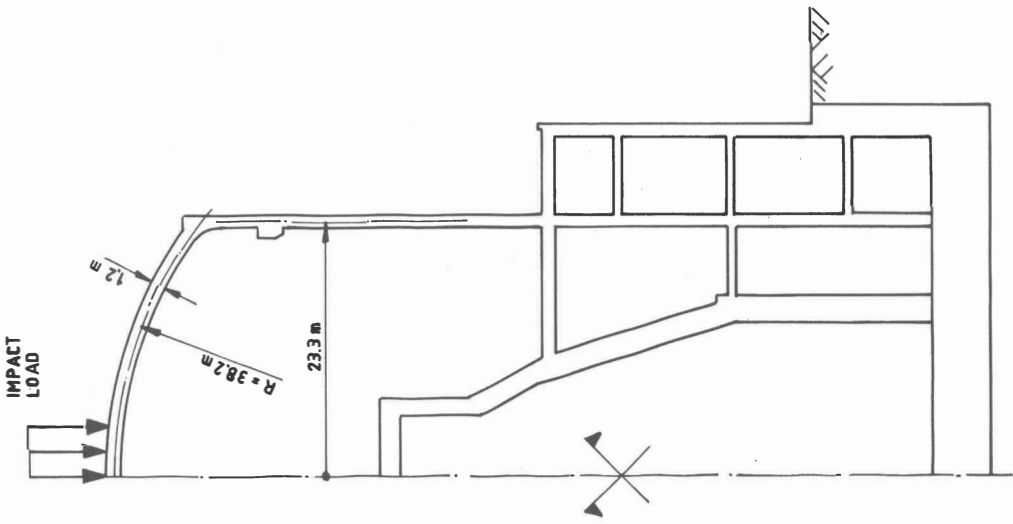


Fig. 2. a) Load-Time-History (Boeing). b) Geometry and Boundary Conditions.

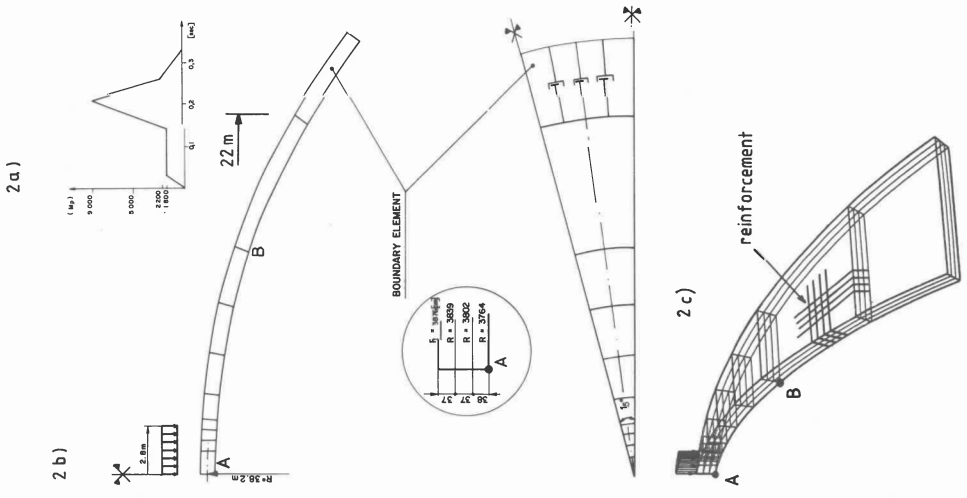


Fig. 1. Impact on Reactor Building

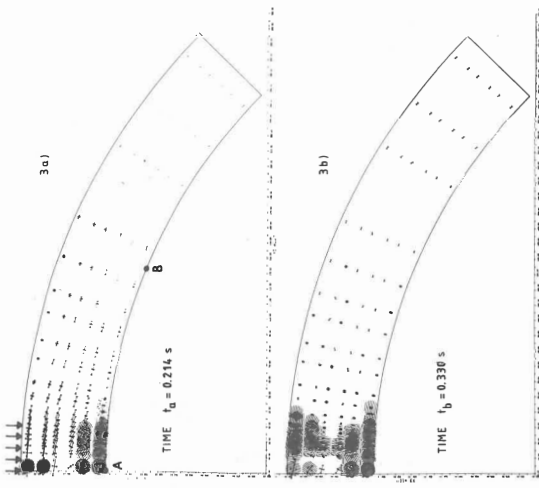


Fig. 3. Principal Stresses and Cracking Patterns (Boeing)

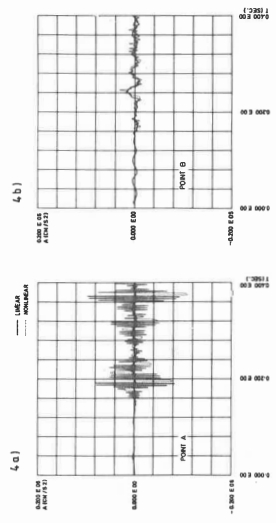


Fig. 4. Acceleration-Time-Histories (Boeing)

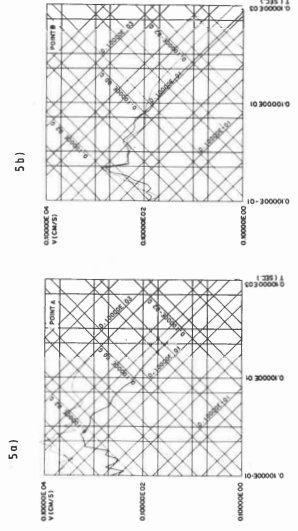


Fig. 5. Response Spectra, 1 % Damping (Boeing)

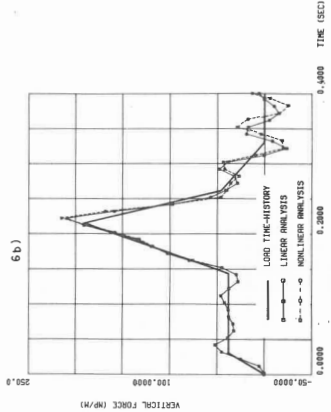
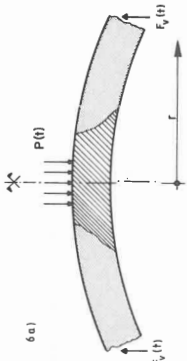


Fig. 6. Vertical Shear Stress-Resultant Time-History (Boeing, $r = 7.5$ m)

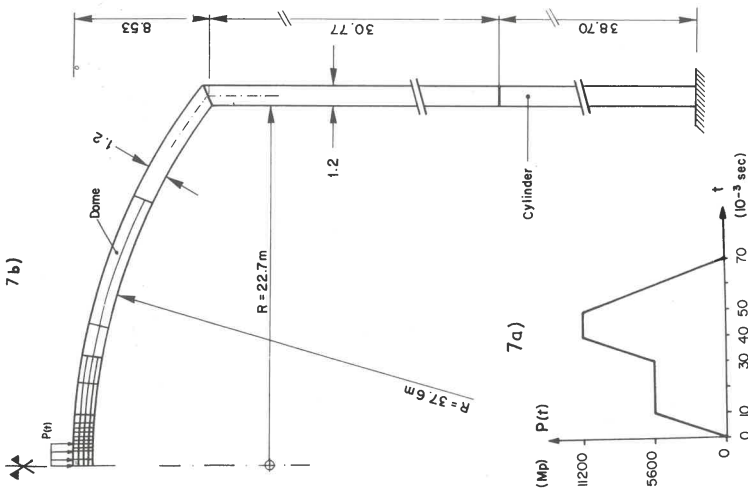
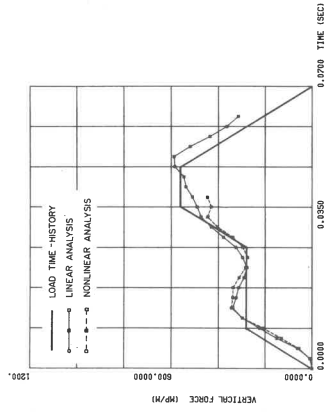
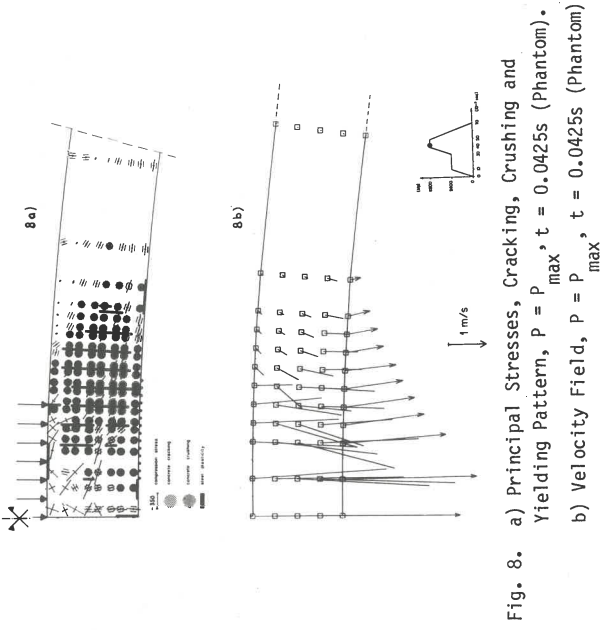


Fig. 7. a) Load-Time-History (Phantom).
 b) Geometry and Boundary Conditions.

Fig. 9. Vertical Shear Stress-Resultant Time-History (Phantom, $r = 3.2$ m, see Fig. 6a)